

횡방향 오염물질 농도 분포 정규성의 거리에 따른 변화

朴 玉 鉉

동아대학교 공과대학 위생공학과
 (접수 1979. 6. 18)

The Variation of Normality of Lateral Impurities Concentration Profile with Distance

Park Ok Hyun

*Department of Sanitary Engineering, College of Engineering,
 Dong-A University, Busan 600-01, Korea*
 (Received June 18, 1979)

요 약

오스트랄리아의 Mt. Isa 에서 3년간 획득된 자료를 이용하여 풍하 장거리(약 1~10시간의 비과시간에 해당하는 거리)에서의 단일 연속연(連續煙)의 횡방향 오염농도 분포에 관한 정규성 가정을 검토하였다. 평탄한 지형에서는 풍하 각 거리에서의 횡방향 오염농도 분포의 비틀림(skewness) 평균치는 영이고, 연속연의 그 비틀림 값은 거리에 따라 현저히 변하지만 영을 중심으로 변화함을 알았다. 그 농도 분포들은 정규분포보다 약간 평탄하며 연이 지표보다 높은 고도를 비과하는 한 그 농도분포들의 평탄도는 지형에 의해 현저한 영향을 받지 않는 것 같다. 풍하 장거리에서의 단일 연속연의 횡방향 오염물질 농도 분포에 관한 정규성 가정은 통계적으로 받아들일 수 있다고 본다.

Abstracts

The Gaussian assumption on lateral impurities concentration distribution of continuous single-plume at long distances on mesoscale is examined with data obtained at Mt. Isa, Australia for 3 years. In flat terrain the average of skewness of lateral impurities concentration profiles at various distances is zero and the value of skewness for successive plume varies significantly with distance but varies around zero. The profiles are somewhat flatter than Gaussian distribution. The kurtosis of them appears not to be significantly affected by terrain as long as plumes

travel at high level compared with surface. The Gaussian assumption on lateral impurities concentration distribution of continuous single plume on the mesoscale may be statistically acceptable.

1. Introduction

Dispersion models do not yet include comprehensive mesoscale meteorological features.¹²⁾¹³⁾

As well known, K theory, similarity theory and statistical theory expressing lateral dispersion of atmospheric pollutants are based on assumptions of steady state conditions, homogeneous flow and statistical Gaussian forms for the lateral distribution of pollutants.¹¹⁾¹⁶⁾ However, steady state conditions of diffusion do not pertain over long time period and some treatments based on an assumption of steady state condition may not be applied in mesoscale diffusion.

Vertical plume concentration distribution has been found to become more flatter as the travel distance increases.⁹⁾¹²⁾

Though a careful analysis of the Project Prairie Grass data by Barad, M.L. and D.A. Haugen(1959)¹¹⁾ has indicated that significant departures from Gaussian concentration distributions do occur, as a practical matter the Gaussian assumption on lateral concentration distribution at short distances is acceptable.⁶⁾⁸⁾

However, the variation of normality of lateral impurities concentration profile with distance has not been generalized yet.

This paper concentrates on the generalization of variation of normality of lateral concentration profile of continuous plumes with distance.

2. Literature review

The profiles of nuclear clouds taken in the

range 1,000 to 1,760 n.mi. at altitude 8,000~15,000 feet above mean sea level were found to be very nearly Gaussian-shaped out to at least 3σ , at which point the radioactivity would be only one % of the peak.¹⁵⁾

Hinds, W.T.(1970)¹⁰⁾ found that through a series of plume diffusion studies in relatively mountainous terrain in California in the range of 1 to 10 km, the average kurtosis of the lateral plume concentration distribution was 3.1, compared to the Gaussian value of 3.0, whereas, the average skewness of the plumes was 0.65, compared to the Gaussian value of zero.

Brown, R.N. et al(1972)²⁰⁾ found that a shearing action of wind tends to elongate and tilt or skew stable palls at distances 10 km and the wind shear action was strong enough to separate palls into cells at a distance 50 km.

The more or less homogeneous structure of the palls changed radically beyond 20 km and there were appreciable variations in the concentration distribution within the palls.

According to Whaley, H. et al(1976),¹⁴⁾ under an elevated inversion continuous plume during normal operation of plant was single one having uniform lateral concentration profiles, while batch plume during emergency flaring was bifurcated one having dual layered concentration profiles.

The normality of lateral concentration profile was found to be independent of wind velocity for neutral atmospheric stability.²⁾

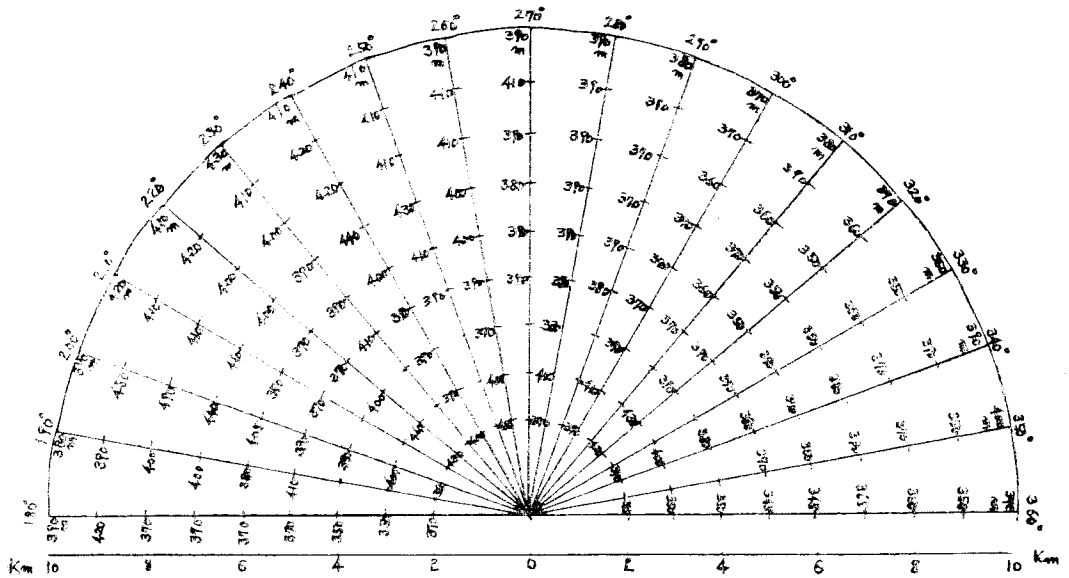


Fig. 1. Altitude within 10 km from source in various wind bearing.

Table 1. Altitude at every 10 km distance in various wind bearing

Dist. (km) Bearing(°)	Dist. (km)				Dist. (km) Bearing(°)	Dist. (km)			
	20	30	40	50		20	30	40	50
220	410 m	390 m	350 m	310 m	270	380 m	350 m	320 m	310 m
230	400 m	390 m	350 m	310 m	280	400 m	350 m	340 m	310 m
240	490 m	370 m	330 m	310 m	290	380 m	350 m	360 m	330 m
250	390 m	350 m	340 m	310 m	300	380 m	370 m	390 m	330 m
260	410 m	370 m	330 m	310 m	310	380 m	370 m	350 m	330 m

3. Terrain

3.1. Distribution of altitude of plume study area

Altitude within 10 km from source and that at every 10 km distance in various wind bearing are expressed in Fig. 1 and Table 1.

Terrain over 50 km from source is similar to that within 50 km.

3.2 Effective roughness length

The dispersion coefficients depend on the aerodynamic roughness of the surface, but no convenient method exists for determining this relationship.¹²⁾

Anyhow the effective roughness length(the roughness length which homogeneous terrain would have in order to produce the correct space average downward flux of momentum near the ground, with a given wind near the

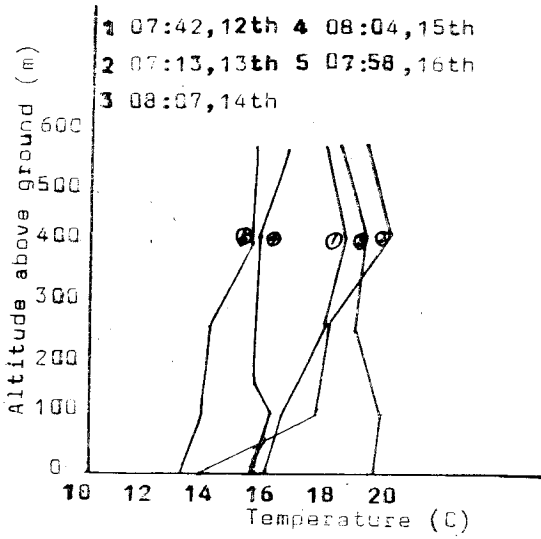


Fig. 2-1 Vertical Temperature Distribution in May, 1975

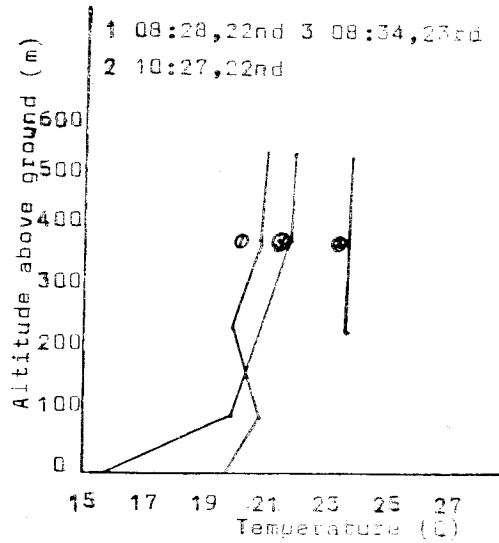


Fig. 2-2 Vertical Temperature Distribution in July, 1975

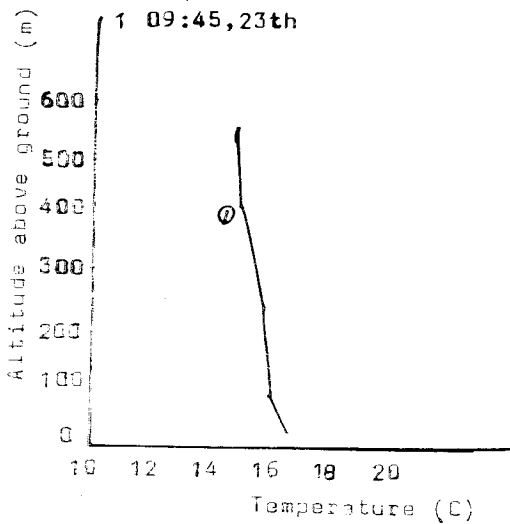


Fig. 2-3. Vertical Temperature Distribution in June, 1976

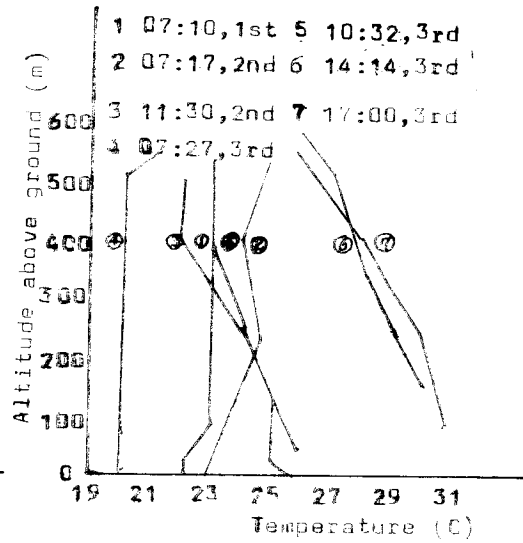


Fig. 2-4. Vertical Temperature Distribution in Sept., 1976

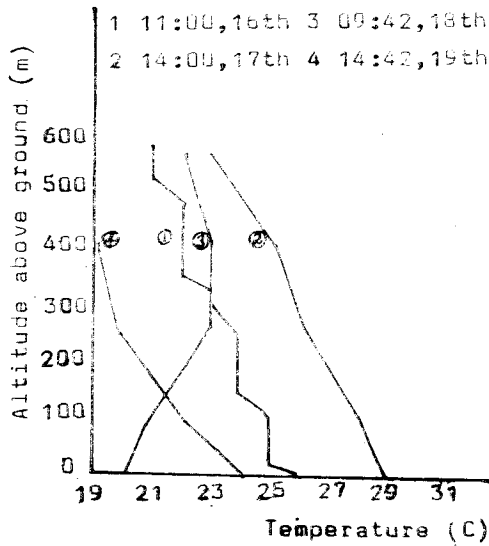


Fig. 2-5. Vertical Temperature Distribution in June, 1977

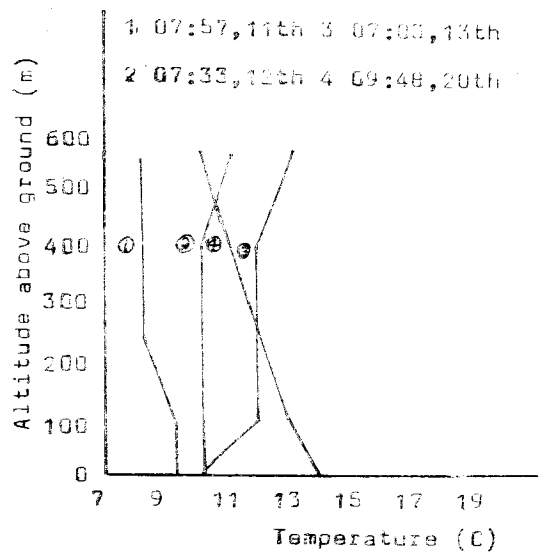


Fig. 2-6. Vertical Temperature Distribution in June, 1977

ground) of the plume survey area may range 0.42(plains) to 0.99(low mountain).⁷⁾

insolation and wind speed at 10 m height and are listed in Table 2.

4. Stability and synoptic weather

4.1 Stability

4.1.1 Vertical temperature distribution

Vertical temperature profile at plume survey area obtained by using a helicopter are as shown in Fig. 2-1~Fig. 2-6.

4.1.2 Mixing height

Figures of the height of inversion layer at night, obtained with acoustic sounder, are as shown in Fig. 3.

4.1.3 Pasquill's stability

Pasquill's stability classes during daytimes were determined by the available data of

4.2 Synoptic weather maps

Synoptic weather maps on days when diffusion experiments were conducted over 10 km distance are shown in Fig. 4-1~Fig. 4-13.

Above maps were taken from "Monthly Weather Review(Queensland)".

High pressure systems locate around Mt. Isa, plume survey area on all experiment days and it should be noted that subsidence inversion may take place in such cases.

5. Lateral dispersion data and the normality of lateral impurities concentration profiles

Lateral short term impurities concentration

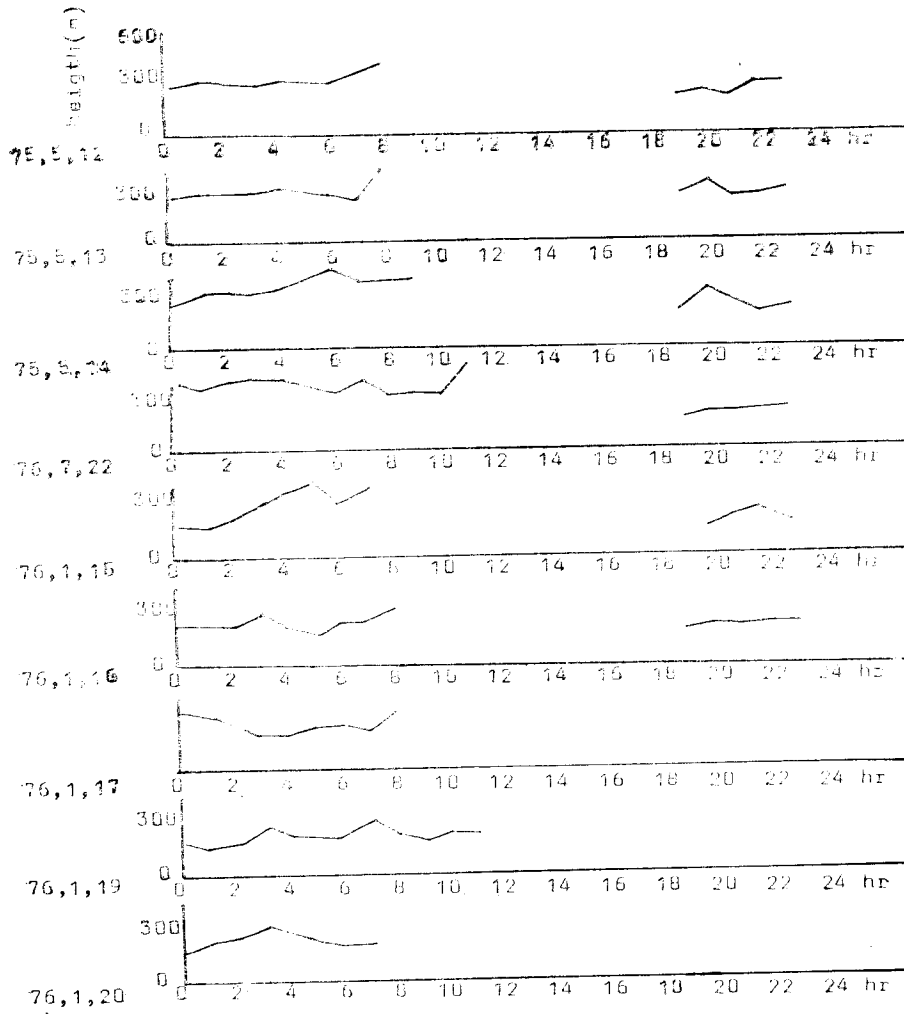


Fig. 3 1. Mixing Height

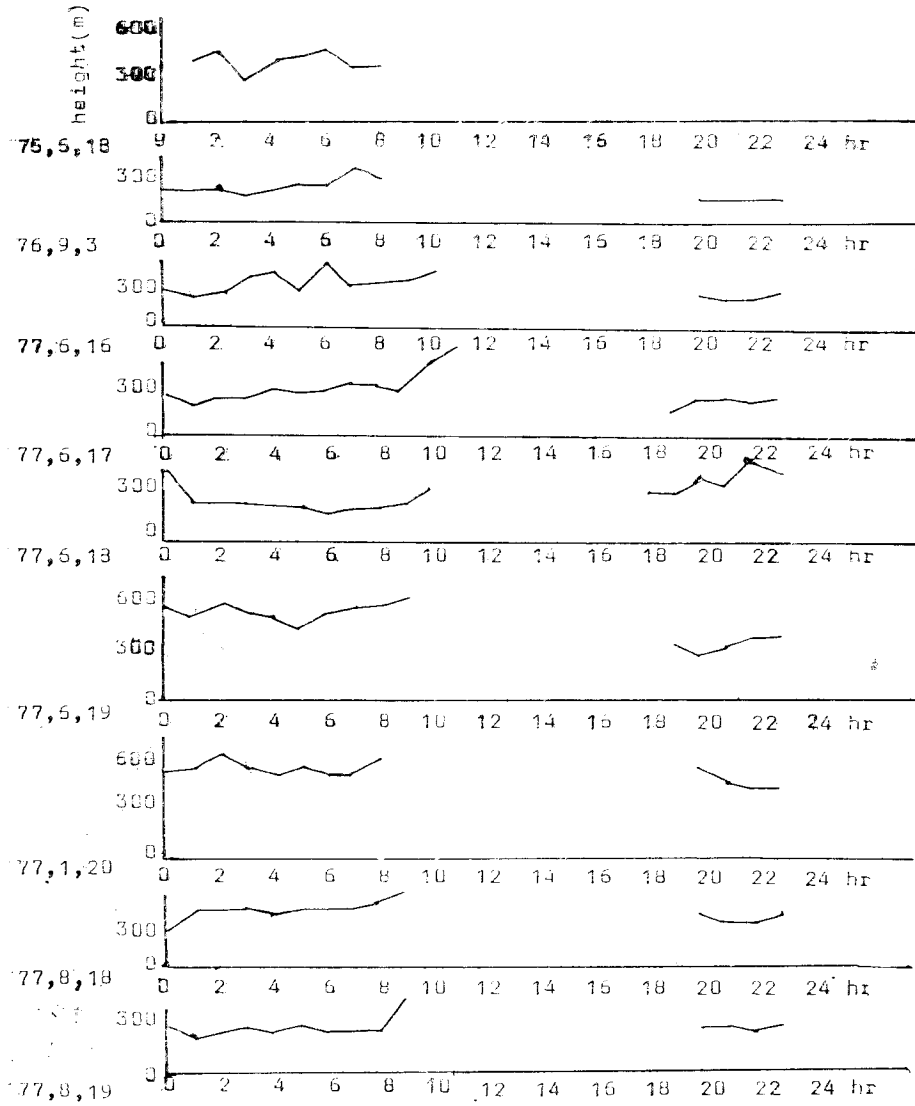


Fig. 3-2. Mixing height

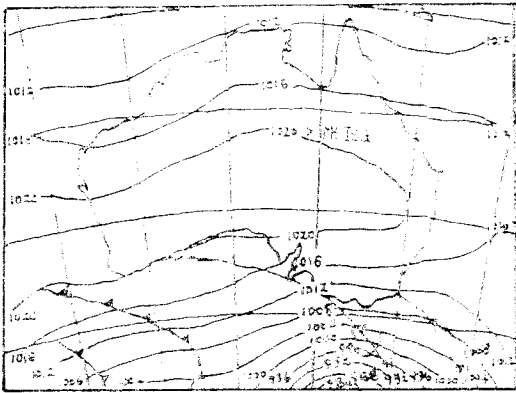


Fig. 4-1. Synoptic weather map on 12th, May, 1975

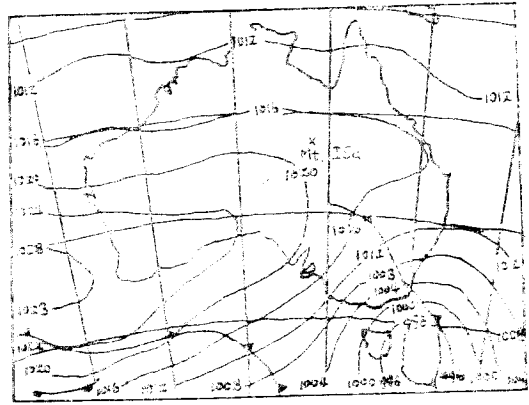


Fig. 4-2. Synoptic weather map on 14th, May, 1975

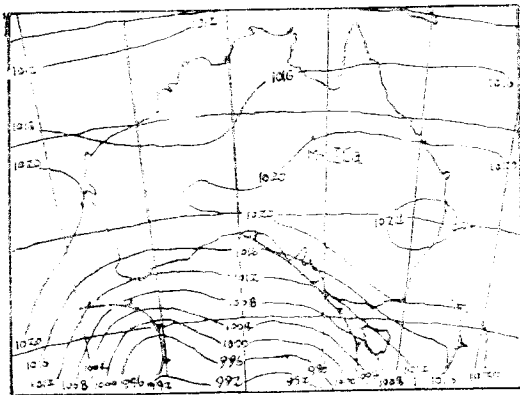


Fig. 4-3. Synoptic weather map on 22nd, July, 1975

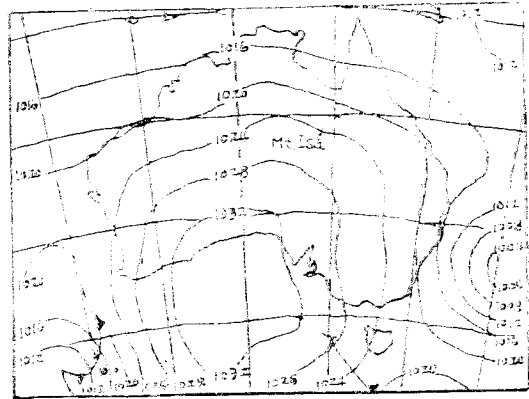


Fig. 4-4. Synoptic weather map on 16th, June, 1976

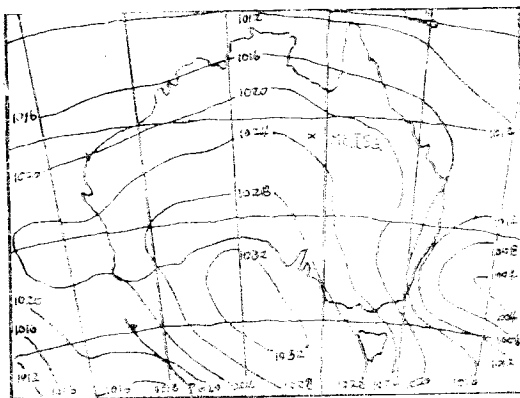


Fig. 4-5. Synoptic weather map on 17th, June, 1976

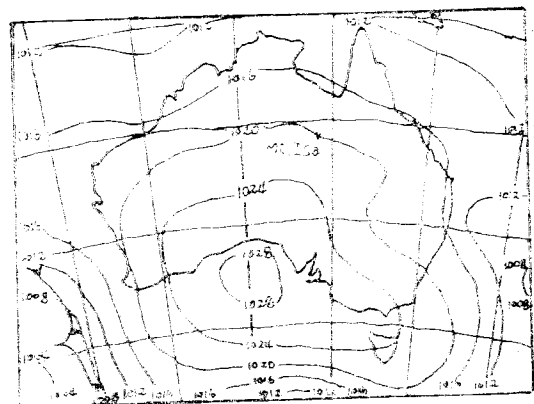


Fig. 4-6. Synoptic weather map on 18th, June, 1976

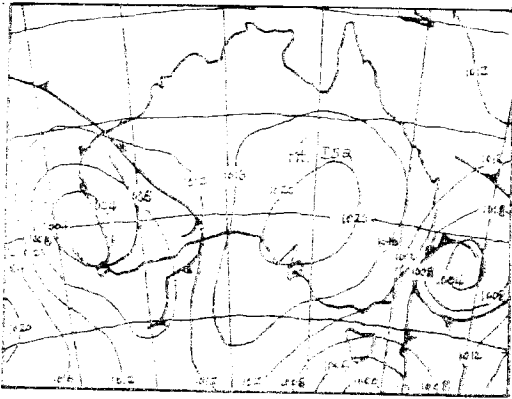


Fig. 4-7. Synoptic weather map on 3rd, Sep., 1976

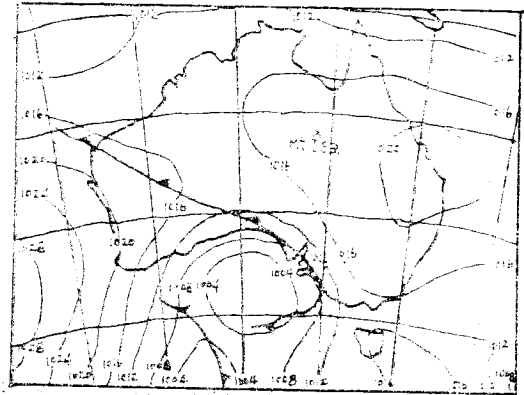


Fig. 4-8. Synoptic weather map on 17th, June, 1977

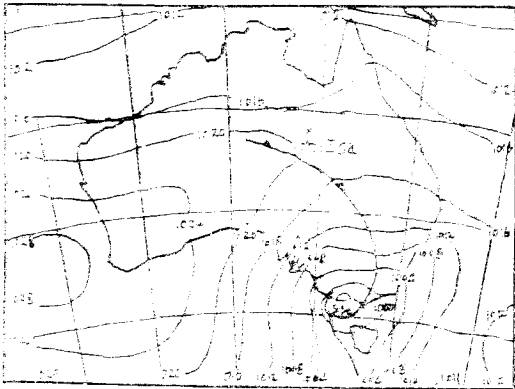


Fig. 4-9. Synoptic weather map on 18th, June, 1977

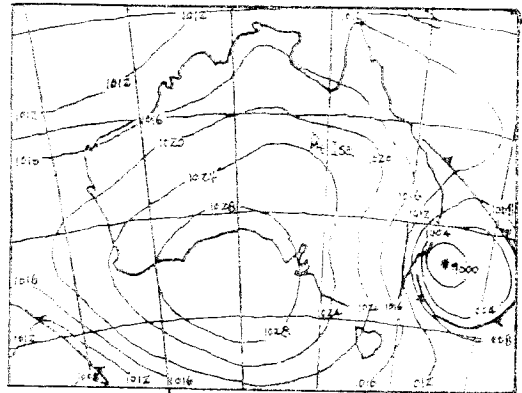


Fig. 4-10. Synoptic weather map on 19th, June, 1977

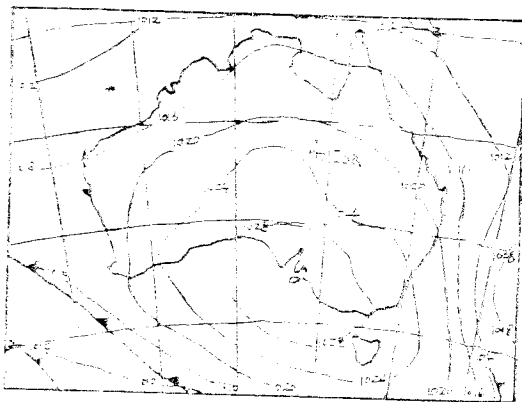


Fig. 4-11. Synoptic weather map on 20th, June, 1977

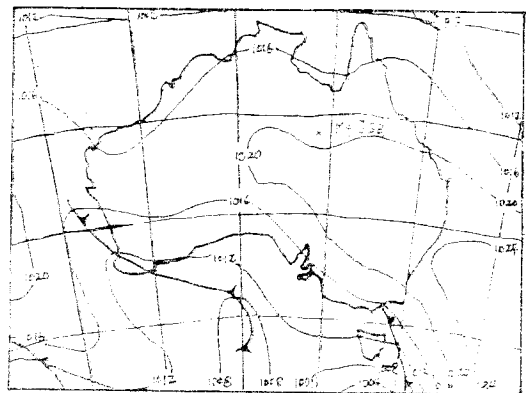
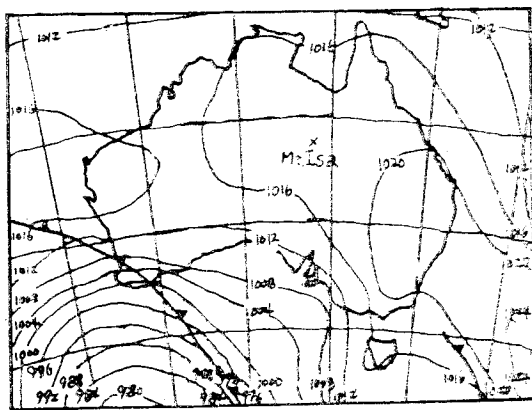


Fig. 4-12. Synoptic weather map on 18th, Aug., 1977

Table 2. Pasquill's Stability Classes

Time	03 AM	09 AM	10 AM	11 AM	12 AM	1 PM	2 PM	3 PM	4 PM	5 PM	6 PM
Date											
76.1.16										D	D
1.17	D	D	D	D	D	D	D	D	D	D	D
1.19								D	D	D	D
1.20	D	D	D	D	D	D	D	D	D	D	D
77.6.16	D	A-B	D	C	C	C	C	B-C			
6.17	E	A-B	D	C	C	C	C	D	C-D	E	D
6.18				B-C	B	D	D	D	D	D	
6.19	D	D	D	C	C	C	C	D	D	D	
6.20	D	D	D	D	C	C	D	D	D		



Scale; 500 km

Fig. 4-13. Synoptic weather map on 19th. Aug., 1977.

profiles were obtained by using COSPEC (Correlation Spectrometer), Nephelometer or TSM (Total Sulphur Meter) mounted in a plane or a car. The standard deviations of lateral spread of plumes, σ_y , were calculated by using equation(1). In order to test the normality of lateral impurities concentration profiles skewness, r_1 and excessive kurtosis, r_2 were calculated by using equation(2) and equation(3) respectively.

$$\sigma_y = \sqrt{\frac{\sum (x_i - \bar{x})^2 \cdot c_i}{\sum c_i}} \quad (1)$$

where x_i =lateral distance from an end of plume.

c_i =impurities concentration.

$$r_1 = \frac{\mu_3}{\mu_2^{1.5}} \quad (2)$$

where $\mu_2 = \frac{\sum (x_i - \bar{x})^2 \cdot c_i}{\sum c_i}$

$$\mu_3 = \frac{\sum (x_i - \bar{x})^3 \cdot c_i}{\sum c_i}$$

$$r_2 = \frac{\mu_4}{\mu_2^2} - 3 \quad (3)$$

where $\mu_4 = \frac{\sum (x_i - \bar{x})^4 \cdot c_i}{\sum c_i}$

Calculation results for distances over 10 km. are listed in **Table 3-1~Table 3-5.**

6. Analysis of data

6.1 Variation of skewness of lateral impurities concentration profiles with distance

Average value of skewness of 63 lateral concentration profiles is about 0.1 as shown in *Fig. 5*, and it appears to be attributable to nearly ideally flat terrain where friction

Table 3-1. Dispersion data and normality of lateral impurities concentration profile

Date	Time	Plume bearing (°)	Distance from source (km)	Altitude of traverse (km)	Sampling time (min.)	Equipment employed	σ_y (km)	r_1	r_2
1975.5.12	08:28	295	38.8	0.25	1.6	Nephelometer	0.87	-0.08	-0.80
1975.5.14	08:30	310	11.0	0.18	0.4	Nephelometer	0.25	-0.43	-0.65
	08:38	318	11.7	0.08	0.5	COSPEC	0.31	0.50	-0.61
	08:42	317	25.1	0.20	0.5	COSPEC	0.27	-0.01	-0.53
	08:51	265	13.1	0.08	0.8	COSPEC	0.55	-0.54	0.70
1975.7.12	09:02	260	31.1	0.03	1.8	COSPEC	0.85	1.06	1.23
	09:13	260	69.0	0.03	2.0	COSPEC	1.19	0.45	-0.41
	10:05	265	109.0	0.03	2.5	COSPEC	1.67	0.21	0.96
	10:53	260	154.0	0.03	5.0	COSPEC	2.50	0.70	-0.55
1976.6.16	11:14	250	33.0	0.12	1.9	TSM	1.19	0.19	-0.88
	11:55	235	107.2	0.12	3.0	TSM	1.84	0.10	-0.88
	12:10	235	107.1	0.12	3.5	TSM	2.15	-0.11	-0.56
1976.6.17	10:15	302	51.8	0.12	1.5	COSPEC	0.87	0.60	-0.40
	10:22	305	52.1	0.28	1.7	COSPEC	1.23	-0.47	-0.31

Table 3-2. Dispersion data and normality of lateral impurities concentration profile

Date	Time	Plume bearing (°)	Distance from source (km)	Altitude of traverse (km)	Sampling time (min.)	Equipment employed	σ_y (km)	r_1	r_2
1976.6.17	10:30	303	50.8	0.45	1.7	COSPEC	1.42	0.45	-0.70
	10:48	300	23.2	0.18	1.3	COSPEC	0.71	0.22	-0.94
	10:56	302	23.4	0.45	1.3	COSPEC	0.88	0.02	-0.75
	11:18	306	20.3	0.15	1.2	COSPEC	0.65	-0.11	-0.82
1976.6.18	09:27	305	24.3	0.15	1.3	COSPEC	0.76	0.82	-0.20
	09:31	298	23.8	0.28	1.2	COSPEC	0.69	-0.28	0.17
	09:36	304	24.5	0.45	1.4	COSPEC	0.62	0.64	0.11
1976.9.3	11:00		23.0	0.32		COSPEC	10.11	-0.59	-1.00
	14:00		23.0	0.55		COSPEC	3.66	-0.02	-0.62
	17:00		230.0	0.83		COSPEC	4.06	-0.02	-0.61
	17:00		230.0	0.83		COSPEC	6.00	-0.04	-0.48
1977.6.16	13:03	223	84.3	0.08	4.0	COSPEC	2.52	0.09	-0.72
	13:22	210	35.0	0.17	2.0	COSPEC	1.21	0.23	-0.92

force is very small.

Fig. 6 indicates that the skewness of lateral impurities concentration profile of successive plume significantly varies with distance but moves around zero.

6.2 Variation of kurtosis of lateral impurities concentration profiles with distance

Average value of kurtosis of 115 lateral

Table 3-3 Dispersion data and normality of lateral impurities concentration profile

Date	Time	Plume bearing (°)	Distance from source (km)	Altitude of traverse (km)	Sampling time (min.)	Equipment employed	σ_y (km)	r_1	r_2
1977 6.17	14:22	210	35.0	0.17	2.0	COSPEC	1.99	0.39	-0.69
	14:45	230	89.5	0.15	7.0	COSPEC	4.65	0.15	-0.87
	15:08	225	139.1	0.08	11.5	COSPEC	8.44	0.39	-0.88
	15:22	233	135.5	0.25	10.5	COSPEC	7.63	-0.48	-0.73
	16:50	230	89.5	0.08	7.0	COSPEC	4.34	0.22	-0.65
	17:07	230	52.5	0.12	3.3	COSPEC	1.56	-0.03	-0.13
	17:17	230	35.9	0.22	2.5	COSPEC	1.99	0.57	-0.83
1977 6.18	11:30	305	96.1	0.28	6.0	TSM	4.13	0.97	0.53
1977 6.19	15:10	325	57.7	0.32	5.8	TSM	3.60	0.38	-0.33
	15:35	330	114.3	0.13	7.0	TSM	4.73	0.16	-0.81
	16:15	325	182.4	0.37	10.0	TSM	5.82	0.40	-0.63
	16:30	320	182.0	0.36	10.0	TSM	5.81	0.13	-0.65

Table 3-4 Dispersion data and normality of lateral impurities concentration profile

Date	Time	Plume bearing (°)	Distance from source (km)	Altitude of traverse (km)	Sampling time (min.)	Equipment employed	σ_y (km)	r_1	r_2
1977 6.19	16:45	320	182.0	0.36	10.0	TSM	6.39	0.23	-0.77
1977 6.20	16:15	320	89.5	0.23	7.5	TSM	4.88	0.96	-0.85
	11:10	320	185.7	0.38	20.0	TSM	13.82	-0.03	-0.83
1977 8.18	16:43	255	53.3	0.55	7.5	TSM	5.82	0.47	-0.58
	17:00	310	42.0	0.55	5.5	TSM	4.02	0.28	-0.63
	17:15	268	40.2	0.55	6.0	TSM	3.78	-0.01	-0.54
	17:25	327	41.3	0.55	5.0	TSM	3.08	-0.04	-0.24
1977 8.19	11:16	290	17.7	0.55	5.5	TSM	3.69	-0.62	0.32
	11:39	280	25.4	0.55	5.5	TSM	3.71	-0.12	-0.32
	11:36	240	25.9	0.55	4.5	TSM	3.36	0.00	-0.62
	11:45	280	34.6	0.55	5.5	TSM	4.07	-0.09	-0.64
	11:52	240	35.1	0.55	6.0	TSM	4.19	0.06	-0.45

concentration profiles is around -0.5 as shown in Fig. 7, which means that the profiles are generally flatter than Gaussian distribution.

Considering the results of Hinds, W.T. (1970),¹⁰⁾ the kurtosis of lateral impurities concentration profile appears to be significantly

affected by atmospheric condition rather than terrain.

Fig. 8 appears to indicate that the variation of kurtosis of lateral concentration profiles of successive plume is not so acute, but further confirmation may be needed.

Table 3-5 Dispersion data and normality of lateral impurities concentration profile

Date	Time	Plume bearing (°)	Distance from source (km)	Altitude of traverse (km)	Sampling time (min.)	Equipment employed	σ_y (km)	r_1	r_2
1977 8.19	12:02	283	43.99	0.55	6.0	TSM	4.93	0.15	-0.80
	12:15	235	26.73	0.55	4.5	TSM	3.67	0.27	-0.66
	12:47	255	14.40	0.55	4.5	TSM	3.39	0.07	-0.91
	14:38	305	19.90	0.55	6.5	TSM	4.84	0.84	-0.74
	14:48	310	22.50	0.55	7.0	TSM	5.47	0.43	-0.45
	15:06	310	37.30	0.55	9.0	TSM	6.37	-0.05	-0.80
	15:20	300	38.80	0.55	8.5	TSM	6.26	0.21	

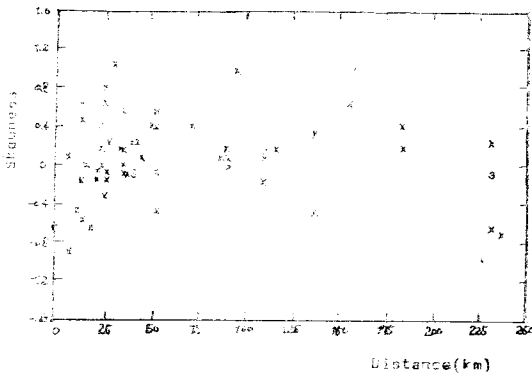


Fig. 5. Skewness data at various distances

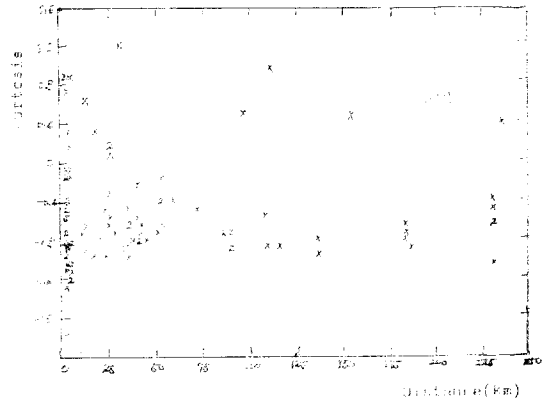


Fig. 7. Kurtosis data at various distances

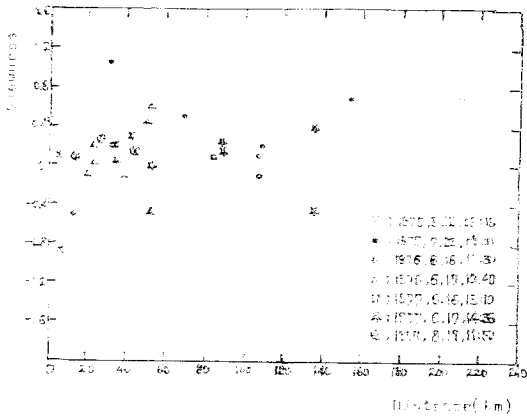


Fig. 6. The variation of skewness of successive plume with distance

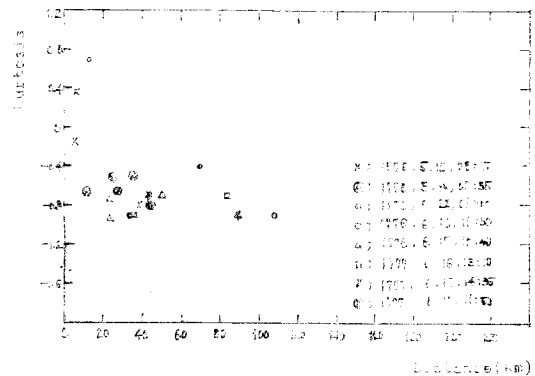


Fig. 8. The variation of kurtosis of successive plume with distance

6.3 Normal probability plot of cumulative plume concentration

In order to generalize the normal probability of lateral concentration distribution, vertical axis is expressed in terms of σ_y and horizontal axis is expressed as cumulative % of concentrations within stated σ_y and an end of plume.

For showing the general tendency of normal probability plot of laterally cumulative plume concentration, it seems essential to average the data plotted as shown in Fig. 9-1~Fig. 9-5.

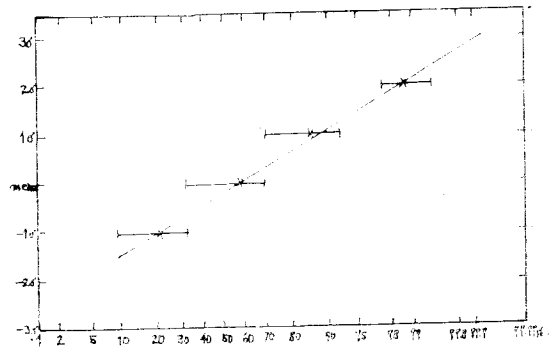


Fig. 9-3. Normal probability plot of cumulative plume concentration in the range 40 to 80 km from source

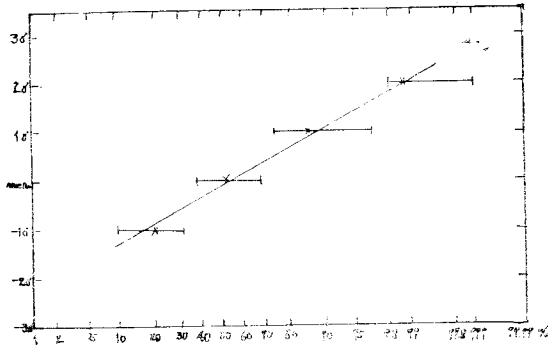


Fig. 9-1. Normal probability plot of cumulative plume concentration in the range 10 to 20 km from source

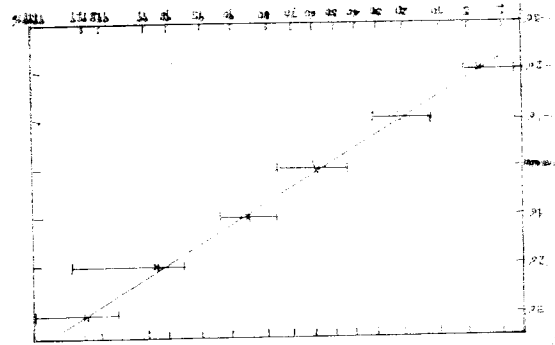


Fig. 9-4. Normal probability plot of cumulative plume concentration in the range 80 to 160 km from source

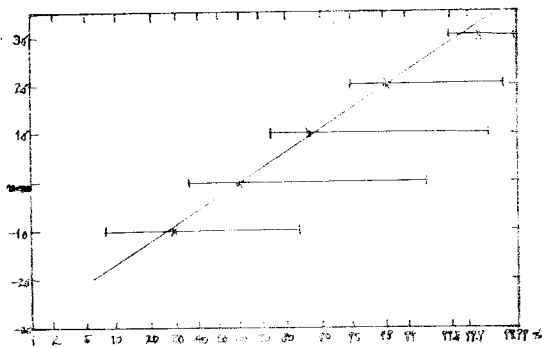


Fig. 9-2. Normal probability plot of cumulative plume concentration in the range 20 to 40 km from source

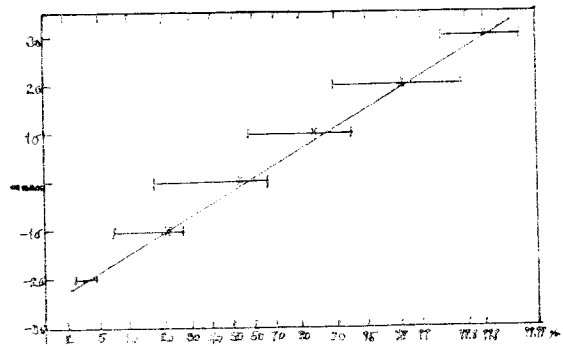


Fig. 9-5. Normal probability plot of cumulative plume concentration in the range 160 to 320 km from source

From Fig. 5, Fig. 7 and Fig. 9-1~Fig. 9-5 it may be concluded that regardless scale of dispersion lateral impurities concentration profile of single plume is statistically Gaussian.

7. Conclusion

1) In flat terrain the average of skewness of lateral impurities concentration profiles at various distances is zero and the value of skewness for successive plume varies significantly with distance but varies around zero.

2) Lateral impurities concentration profiles are generally somewhat flatter than Gaussian distribution.

The kurtosis of them appears not to be significantly affected by terrain as long as plumes travel at high level compared with surface.

3) The statistically Gaussian assumption on lateral impurities concentration distribution of continuous single plume may be acceptable regardless the scale of dispersion. Therefore diffusion equation to be used for calculating pollutants concentration at distances on the mesoscale where vertical impurities concentration profile is flat may be;

$$C \propto \frac{1}{\sqrt{2\pi}\sigma_y} \exp\left[-\frac{1}{2}\left(\frac{y^2}{\sigma_y^2}\right)\right]$$

$$\therefore C = \frac{Q}{\sqrt{2\pi}\sigma_y \cdot U \cdot H} \exp\left[-\frac{1}{2}\left(\frac{y^2}{\sigma_y^2}\right)\right]$$

- where C =pollutants concentration in g/m^3
- σ_y =diffusion coefficient in y direction in m
- Q =the fraction of pollutants staying within mixing height in g/sec .
- U =average wind speed in m/sec
- H =mixing height in m

Acknowledgement

The author wishes to express appreciation to C.S.I.R.O. scientists named Mr. D. Williams, Mr. J. Millne, and Mr. D. Robert who gave me raw data which they had vitally contributed to collection. The author also wishes to thank Dr. M.F.R. Mulcahy of C.S.I.R.O. and associate professor E.T. Linacre of Macquarie University who helped me so that this research can be conducted.

This paper was made by help with finance supported by Dong-A University.

References

1. Barad, M.L. and D.A. Haugen(1959). A preliminary evaluation of Sutton's hypothesis for diffusion from a continuous point source. *J. Meteor.* Vol. 16, pp.12~20.
2. Brown, R.N., L.A. Cohen and M.E. Smith (1972). Diffusion measurements in the 10 ~100 km range. *J. App. Meteor.*, pp.323 ~334.
3. Commonwealth of Bureau of Meteorology, Australia(1975). *Monthly Weather Review* (Queensland). May. July.
4. Commonwealth of Bureau of Meteorology, Australia(1976). *Monthly Weather Review* (Queensland). June. Sept.
5. Commonwealth of Bureau of Meteorology, Australia(1977). *Monthly Weather Review* (Queensland). June. Aug.
6. Cramer, H.E. (1959). Engineering estimates of atmospheric dispersal capacity. *Amer. Industrial Hygiene Ass. J.* Vol. 20, pp.183 ~189.
7. Fiedler, F. and H.A. Panofsky(1972). The geostrophic drag coefficient and the effective roughness length. *Int. J. Royal Meteorological Society.* Vol. 98, pp.213~200.
8. Gifford, F.A.(1960). Atmospheric dispers-

- ion calculations using the generalized Gaussian plume model. Nuclear Safety. Vol. 2, No. 2, pp. 56~69.
9. Gillani, N.V., R.B. Husar, J.D. Husar, D.E. Patterson and W.E. Wilson, Jr.(1978). PROJECT MISTT; Kinetics of particulate sulfur formation in a power plant plume out to 300 km. Atmos. Env. Vol. 12, pp. 589~598.
 10. Hinds, W.T.(1970). Diffusion over coastal mountains of southern California. Atmos. Env. Vol. 40, pp. 107~124.
 11. Pasquill, F.(1974). Atmospheric diffusion. London.
 12. Ragland, K.W. and R.L. Dennis(1975). Point source atmospheric diffusion model with variable wind and diffusivity profiles. Atmos. Env. Vol. 9, pp. 179~189.
 13. Wallington, C.E.(1975). Calculation of atmospheric dispersion. Proc. of 5th Int. Clean Air Conference. pp.381~402. Rotorua.
 14. Whaley, H.G., K. Lee and J.G. Gainer (1976). Plume dispersion from a natural gas sulphur extraction plant under a persistent elevated inversion. Proc. of 13th World Gas Conference. London.
 15. Wilkins, E.M.(1958). Effective coefficients of diffusivity for atomic bomb clouds at one to two thousand miles. Transaction. American Geophysical Union. Vol. 39, pp. 58~59.
 16. World Meteorological Organization(1972). Dispersion and forecasting of air pollution. WMO Tech. Note 121, p. 13.